Microradiographic Observation of the Strain Field in Vicinity of the Crack Tip

Daniel Vavřík[1,2*] **,** Ivan Jandejsek[1], Jan Jakůbek[2], Martin Jakůbek and Tomáš Holý[2]

[1] Institute of Theoretical and Applied Mechanics, v.v.i. of the Czech Academy of Sciences, Prosecka 76, Prague 9, Czech Republic

[2] Institute of Experimental and Applied Physics of the Czech Technical University in Prague, Horska 3a/22, 128 00, Prague 2, Czech Republic

[*] E-mail: vavrik@itam.cas.cz

Keywords: Strain Measurement, Digital Image Correlation, X-ray radiography, Ductile Fracture Mechanics

Abstract. Studies concerning ductile fracture mechanics require information about strain field in vicinity of the crack tip. Although it is a quite common problem new challenges occur when we are interested in strain field in micrometric scale, especially in the situation of mixed plane stress-strain mode in vicinity of the crack tip. Measurement of the strain field may be generally done using some markers which can be traced during loading. Micro-radiographically visible structures of alloys or composites can be utilized as such markers.

Introduction

Failures in ductile materials and composites with stress concentrator precede an intensive plastic strain evolution which is followed by internal material damaging. Material damaging is developed in a process zone which has a relatively small dimension. The crack growing is observed when specific level of plastic strain intensity and damaging is reached. Hence, not only the onset and existence of damage and plastic strain but also its quantification and time evolution have to be determined for material science research. Standard numerical models are mostly verified by global behavior of the loaded specimen studied as "Load-displacement record" using known material parameters. Advanced numerical models are moreover supported by some optical methods allowing measurement of the strain field in the specimen surface.

Let's concentrate on a flat geometry of the used specimen. Although globally it can be assumed that such specimen is governed by the plane stress state behavior, mixed stress-strain plane mode can be observed in vicinity of the crack tip. It is a weak point of standard optical methods which are able to measure free specimen surface only on which plane stress state is presented although plane strain state better describes inner material behavior in vicinity of the crack tip. As material damage is processed mostly inside of the material it is usually hard to recognize damage zone from the specimen surface directly by any optical methods. Moreover, in many cases crack is firstly advancing inside of the specimen (crack tunneling) and it cannot be recognized from the surface too.

For the purpose of observation of processing zone behavior and crack growing during specimen loading, the X-ray Dynamic Defectoscopy (XRDD) technique has been developed [1]. XRDD has spatial resolution of the micrometric scale thanks to usage of the microspot X-ray source, high resolution detector system and advanced radiograms data processing. [2]. Radiographically recognizable structures serve for calculation of displacement field done by Digital Image Correlation technique.

The XRDD radiographic technique integrates material behavior through the specimen thickness transmitted, consequently prevailing local stress-strain state is observed by this way. Moreover,

damage evolution is observed simultaneously without losing interconnection of all parameters followed. Displacement and strain fields, plastic strain field, strain work rate and other parameters are calculated in postprocessing phase of experimental data.

X-ray Dynamic Defectoscopy

The principle of the XRDD consists in illuminating of the sample object by X-rays during the loading process and observing real time material behavior. Both in-plane material deformation and thickness specimen reduction are observed simultaneously thanks to a precisely 'measured signal to material thickness' calibration by the Signal to Equivalent Thickness calibration method (SET) [2]. The measured changes in transmission represent alterations of effective thickness of the specimen. The effective thickness changes are understood as weakening of the material by damage volume fraction and by the contraction [1]. In-plane deformations are measured using material microstructure as unique markers for X-ray Digital Image Correlation method (See paragraph below).

Regarding scale of the grain structure and damage zone to be observed, a radiographic spatial resolution of micrometric scale is required. The principal requirements to be fulfilled in order to achieve high spatial resolution in X-ray imaging are: point-like source of X-ray beam and highly efficient X-ray detector with large dynamic range and advanced radiograms postprocessing. We employed an X-ray tungsten microfocus tube with a focal spot of 5 μm and divergent cone point-like source beam which enable a magnification up to the micrometer scale in spatial resolution. As an X-ray detector we used the single X-ray photon counting digital pixelated Medipix-2 device [4]. The so called beam hardening effect arises as a significant source of X-ray image distortion which can be eliminated by the "SET".

X-ray Image correlation

The X-ray image correlation method, which was used for the observation of the loaded body deformations, is based on the same principles as the standard optical image correlation technique. We are looking for self-similar places in a sequence of images acquired during the experiment. The source of experimental data is different, though. The standard image correlation technique is utilizing optical images of the surface which is covered by a contrast speckle spray paint [5]. The X-ray Digital Image Correlation (XDIC) is based on radiographic observation of the natural material structure [6]. For metals, this material structure (pattern) is induced by nonhomogenous distribution of the alloy components as was shown in [7]. The Al-alloy material we used exhibited a "stable" random pattern used for XDIC thanks to the non-homogenous Cooper distribution in this alloy. See Fig. 1 for illustration of such pattern [7].
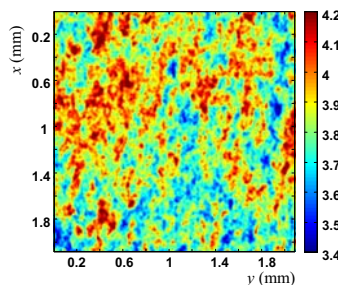

Fig. 1: Cu mass fraction [%] in the Al-alloy specimen.

A sequence of radiographs is taken during the loading experiment. A grid of control points is selected in the first reference radiograph. Positions of these points are searched in the next target

radiograph. The X-ray image correlation uses the following general procedure: a template surrounding the control point is extracted in the reference radiograph for each control-point pair and in the target radiograph at the same coordinates. A normalized cross-correlation of the templates is calculated for this start position and for positions surrounding this point. This way we get a matrix of cross-correlation coefficients. Finally, the absolute sub-pixel peak of the cross-correlation matrix is found using a second order polynomial surface. The peak position is used as coordinates of a new reference control point. The procedure as described is repeated for all radiographs step by step. Each template has to cover a distinguishable structure pattern. Standard used DIC approach using Fast Fourier transformation does not work for material pattern because this pattern has a quite low contrast and too low Signal to Noise Ratio (SNR) [6].

A displacement field obtained from control points tracing is used for a consequent calculation of the fields of the principal strains ε_1 and ε_2. Third principal strain field ε_3 is calculated due to precise measurement of the actual specimen thickness at the same points as first two principal strains are measured using SET method. All principal strains are used for calculation of the equivalent stress field and plastic strain field using incremental theory of the plasticity [9]. The plastic strain energy density rate is calculated as well for the purpose of energy dissipation rate [10].

Thanks to radiogram transmission measurement of the principal strains the dominant strain type is measured regardless whether the deformation type is strain or stress plane.

Experimental setup

The experimental setup consists of the radiographic system, fixed loading equipment and several computer controlled stages, Vavrik *et al.* [6]. The entire setup is placed in a fully shielded box ensuring staff dose safety. The basic concept of the radiographic system is given by the stable position of both the X-ray tube and detector during measurements as well as by the operational movement of the observed object fixed in loading equipment (which is kept fixed with a supporting frame to the computer controlled motorized stage). Two disc holders of calibration filters are employed in the calibration phase with the SET. Each disc carries ten pure Aluminum calibrators, providing together up to one hundred combinations of calibrator thickness values.

For the purpose of radiographic measurements, a new transferable 25 kg and highly stiff loading device has been developed. This device is equipped with four stepper engines ensuring the symmetrical loading of specimens with relatively stable position of the observed area in the X-ray beam. Grips displacement is realized by the screws rotation using stepper motors with harmonic transmission. The resultant transmission ratio is extremely high and allows precise and very slow loading. The loading force is recorded by two load cells while grip displacement is measured by two extensometers. The loading force capacity of the device is 100 kN and weights only 25 kg with dimensions 377x343x190 mm. These parameters allow to fix the loading equipment onto a PC controlled motorized stage during measurements.

Regarding the precision positioning of the observed object, stepper engines are employed for the motorized stage. This stage has two linear axes in the plane perpendicular to the beam direction with 5 μm accuracy and one rotation around the vertical axis with 2 sec accuracy. These axes allow precise positioning of the observed object.

All operational parameters of the experimental setup, the X-ray imaging and post-processing are controlled with the help of one integrated software package. This solution enables to operate and control a number of features and components such as the motorized stage, the parameters and exposition of the X-ray source, the acquisition of X-ray images, the recording data from load cells and extensometers, the positioning of calibrator discs, the acquisition of optical images and the driving of the loading device. The complete system can be fully controlled via USB interface for which in addition interface commands are properly synchronized.

Experimental

The specimen for measurements was prepared from a high-ductile aluminum alloy. Its elastic modulus E was 70 GPa, Yield stress σ_{ys} was 296 MPa and Poisson's ratio μ was *0.315*. The source experimental material had a shape of a thick plate manufactured by the heat rolling technology. The experiment was carried out on a flat specimen 170 mm long, 50 mm wide and 5 mm thick. The central slit pre-machined by spark-out technology was 10 mm long and had 0.3 mm width. The initial 3 mm long precrack was prepared by fatigue loading on both sides of the slit. The fatigue pre-cracks were not exactly perpendicular to the specimen surface. Contrast led marks were glued in the vicinity of the crack tip as contrast reference points.

The specimen was loaded in uni-axial tension by grips displacement with velocity 0.4 μm/sec until initial cracks prolonged to several millimeters. Distances between the X-ray source, the observed specimen and the Medipix-2 detector were set as short as possible to achieve a high number of detected X-ray photons. Consequently, the magnification factor of 3.6 was reached. The complete experiment took 34 min 12 s. A radiographic snapshot with exposure time of 0.5 sec was taken each 0.85 sec (2420 images). Data from extensometers (grips displacement) and from load cells (loading force) were scanned every second.

All X-ray images were processed by the DTC. The resultant map of specimen thicknesses was obtained for each analyzed loading level. Finally, the damage zone and the crack propagation were visible and the internal structure of the specimen was recognizable too.

Results

The recognition of features within the sample is limited by the number detected X-ray photons in each detector's pixel. Therefore, a floating average of forty snapshots was calculated. The sum of the forty snapshots of the slightly loaded specimen, when fatigue precrack was open, is shown in Fig. 2. (pseudocolors are used for a better indication). This radiograph was processed by the SET same as the other radiographs. The red color represents the thickest material (the contrast led marks), the blue color represents the thinnest place of the specimen (it is the crack in the middle between the led marks). The grainy structure of the material is easily recognizable. Even the horizontally oriented grain structure formed by the heat rolling is visible. The fatigue crack tip has coordinates [0,0]. The image has the scale in millimeters. The radiograph of the specimen just before crack growing is in Fig. 3. An intensive 0.7 mm long damage zone was developed in front of the crack tip.
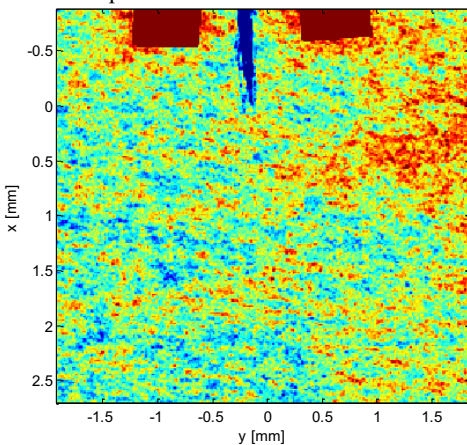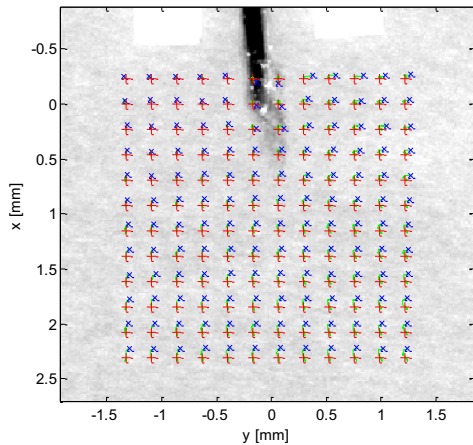
Fig. 2: Radiogram of the specimen   Fig. 3: Tracking paths before crack advancing.

The tracking paths up to actual position are depicted in Fig. 3. The green cross marks represent the initial positions, the blue line paths and the red "x" mark represents the final positions of the control points at the actual loading level. Plastic work rate evolution was calculated for all loading levels in the area of 0.8 mm^2 in front of crack tip (3x5 measuring cells), See fig. 4. This plastic work rate was normalized by the actual specimen thickness. Two significant extremes A and B were observed. Extreme A corresponds to a moment just before first crack advance (see Fig. 3). Extreme B preceded beginning of the faster crack growing, related minimum C was followed.
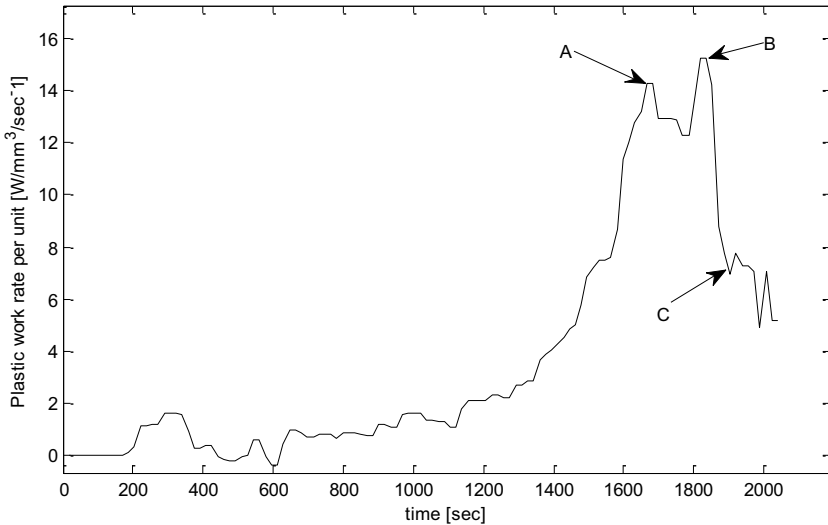
Fig. 4: Plastic work rate per unit in the area in front of the crack tip.

As mentioned above, stress-strain fields and plastic strain intensity were calculated for all loading levels. The plastic strain field corresponding to the extreme A just before crack growing is depicted in the Fig. 5. Related stress intensity field is depicted in the Fig. 6.
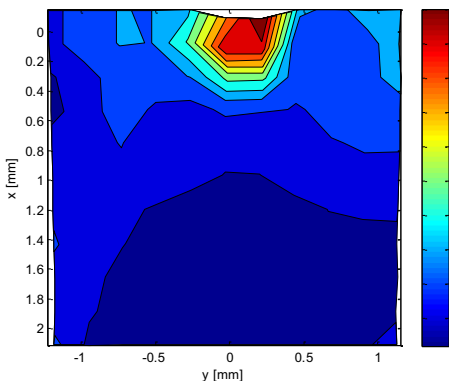

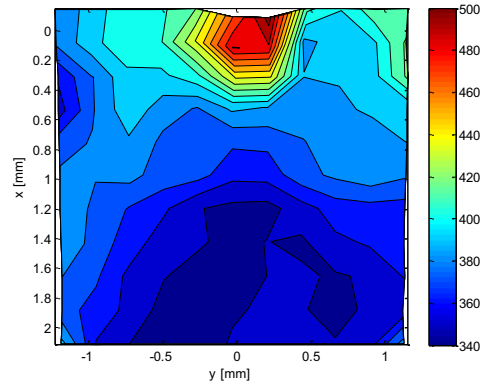Fig. 5: Plastic strain ε_{pl} at the maximum A Fig. 6: Stress intensity σ at the same level A

The plastic strain field corresponding to the extreme B is depicted in the Fig. 7. .Corresponding radiogram is in the Fig. 8 (this image has different graphical scale). Data z axis corresponds to the specimen thickness (see right colorbar). The crack has length 0.3 mm and damage zone has length 0.7 mm.
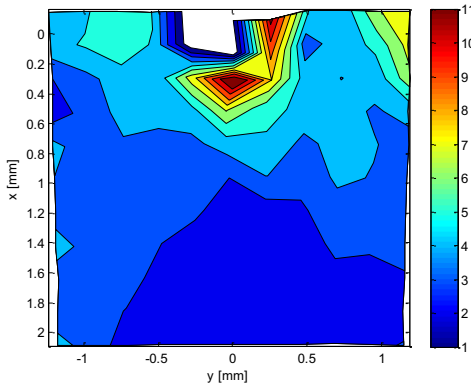
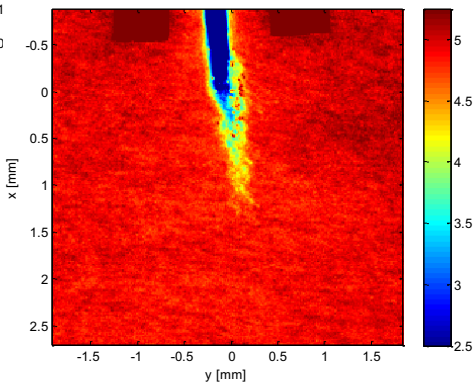Fig. 7: Plastic strain ε_{pl} at the maximum B Fig. 8: The radiogram at the same level B

The plastic strain field corresponding to the local minimum C is depicted in the Fig. 9. Maximum plastic strain intensity is lower than in the previous maximum B, but average intensity in whole area studied is higher. Corresponding radiogram is in the Fig. 10. New crack has length 0.65 mm, related damage zone has length 1.1 mm.
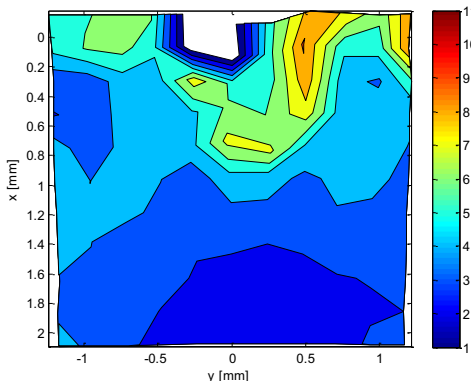

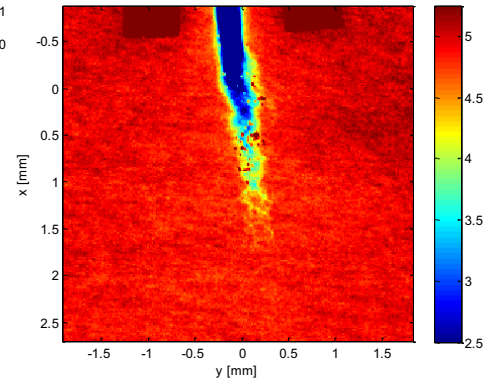Fig. 9: Plastic strain ε_{pl} at the minimum C Fig. 8: The radiogram at the same level C

Conslusions

The X-ray Digital Image Correlation technique for measurement of the all strain components used for consequent calculation of the plastic strain field, stress intensity and plastic strain energy density was successfully realized.

Extremes in the Plastic work rate indicated distinct points of the damage zone and crack evolution during loading.

The measurement of the strain fields using the X-ray image correlation is possible thanks to an excellent quality of the radiographs. The quality arises from the high dynamic range of the X-ray pixel Medipix-2 detector and the Signal to Thickness Correlation method. Even the horizontal orientation of the grain structure which comes from the heat rolling is visible.

The dimensions and shapes of the damage zone and crack are measured directly using X-ray Dynamic Defectoscopy during loading experiment.

Increasing of the resolution and accuracy is still possible with slower loading and/or more intensive X-ray source thanks to increasing of the radiograph data statistic.

Acknowledgments

References

[1] D. Vavřík, J. Jakůbek, S. Pospíšil, J. Visschers: Non-destructive Observation of Damage Processes in Loaded High Ductile Specimens with Different Crack Configuration by X-Ray Dynamic Defectoscopy, Materials Science Forum Vols. 480-481, Trans Tech Publications, Uetikon-Zurich, Switzerland, February 2005,pp. 231-236, ISBN 0-87849-962-8

[2] Jan Jakubek: "Data processing and image reconstruction methods for pixel detectors", in Nuclear Instruments and Methods in Physics Research Section A, 576 (2007) 223-234, NIMA 46615.

[3] S. S. Russell and M. A. Sutton, *Experimental Mechanics*, Vol. **29**, 237-240, 1989

[4] X. Llopart, M. Campbell, R. Dinapoli, D. San Segundo, E. Pernigotti: Medipix2, a 64k pixel readout with 55 μm square elements working in single photon counting mode, IEEE Trans. Nucl. Sci., 49:2279-2283, 2001.

[5] W.H. Peters and W.F. Ranson, Digital imaging techniques in experimental stress analysis, Opt Eng 21, (1982), pp. 427–431.

[6] Vavrik, D., Holy, T., Jakubek, J., Jakubek, M., Bryscejn, J., Tichy, V., Vykydal, Z., Valach, J.: Radiographic observation of damage zone evolution in high ductile specimen, In *Proceedings of the 16th European Conference of Fracture*, edited by E. Gdoutos, Alexandropolis, Greece, Springer, 2007

[7] Holý, T. ; Jakůbek, J. ; Jakůbek, M. ; Valach, Jaroslav. Microradiographic Observation of Grainy Structure of Al alloy. In Microradiographic observation of grainy structure of Al-alloy. Honolulu : IEEE NSS, 2007. S. 1711-1715. ISBN 978-1-4244-0923-5. ISSN 1082-3654.

[8] Vavrik, D., Holy, T., Jakubek, J., Jakubek, M. Valach, J.: Micrometric scale measurement of material structure moving utilizing μ-radiographic technice, NIMA Vol 591/1 pp 24-27, DOI 10.1016/j.nima.2008.03.019

[9] Vavřík, D. & Zemánková, J.: Crack Instability in Ductile Materials Analyzed by the Method of Interpolated Ellipses., *Experimental Mechanics*, Vol. 44, (2004) pp. 327-335

[10] Lee, D. J., Liebowitz, H., Lee, K.Y.: "The Quest of a Universal Fracture Law governing the process of Slow Crack Growth," Engineering Fracture Mechanics, 55, pp.61-83 (1996).